Magnesium Deficiency Causes Loss of Response to Intermittent Hypoxia in Paraganglion Cells*[S]

Satoru Torii[‡], **Kentaro Kobayashi**[‡], **Masayuki Takahashi**[‡], **Kasumi Katahira**[‡], **Kenji Goryo**[‡], **Natsuki Matsushita**[§],
Ken-ichi Yasumoto[‡], **Yoshiaki Fujii-Kuriyama**[¶], and **Kazuhiro Sogawa**[‡1]

From the [‡]Department of Biomolecular Sciences, Graduate School of Life Sciences, Tohoku University, Aoba-ku, Sendai 980-8578, the [§]Department of Biochemistry and Molecular Genetics, Graduate School of Medicine, University of Ehime, Matsuyama 791-0295, and [¶]Center for Tsukuba Advanced Research Alliance and the Solution-Oriented Research for Science and Technology (SORST) Project, Japan Science and Technology Agency, University of Tsukuba, 1-1-1 Tennoudai, Tsukuba 305-8577, Japan

Magnesium deficiency is suggested to contribute to many age-related diseases. Hypoxia-inducible factor 1α (HIF-1α) is known to be a master regulator of hypoxic response. Here we show that hypomagnesemia suppresses reactive oxygen species (ROS)-induced HIF-1α activity in paraganglion cells of the adrenal medulla and carotid body. In PC12 cells cultured in the low magnesium medium and treated with cobalt chloride ($CoCl_2$) or exposed to intermittent hypoxia, ROS-mediated HIF-1α activity was suppressed. This suppression was due to up-regulation of inhibitory PAS (Per/Arnt/Sim) domain protein (IPAS) that was caused by NF-κB activation, which resulted from ROS and calcium influx mainly through the T-type calcium channels. Induction of tyrosine hydroxylase, a target of HIF-1, by $CoCl_2$ injection was suppressed in the adrenal medulla of magnesium-deficient mice because of up-regulation of IPAS. Also in the carotid body of magnesium-deficient mice, $CoCl_2$ and chronic intermittent hypoxia failed to enhance the tyrosine hydroxylase expression. These results demonstrate that serum magnesium levels are a key determinant for ROS-induced hypoxic responses.

Hypoxia-inducible factor 1α (HIF-1α)[2] and its family members are master regulators of hypoxic response (1–3). In hypoxia, the HIF-1, composed of HIF-1α and HIF-1β/Arnt, binds to hypoxia response element (HRE) to induce the gene expression of hypoxia-responsive proteins, such as erythropoietin and vascular endothelial growth factor. In addition to these proteins, tyrosine hydroxylase (TH), the rate-limiting enzyme for catecholamine biosynthesis, is induced in rat pheochromocytoma-derived PC12 cells and paraganglion cells in the adrenal medulla (AM) and carotid body (CB) in response to hypoxia

(4). The CB acts as the primary peripheral chemoreceptor (5), and glomus cells of the CB are responsible for monitoring oxygen levels in arterial blood (5, 6). Through the release of neurotransmitters, including dopamine, the CB delivers information to the respiratory and cardiovascular networks in the brainstem, resulting in increases of ventilatory frequency and volume and also raising cardiac output.

HIF-dependent hypoxic response is also caused by chronic intermittent hypoxia (CIH), which is a common feature of obstructive sleep apnea (OSA). There is accumulating evidence that CIH is associated with an increased oxidative stress (7, 8). Peng *et al.* (9) have shown that CIH induces reactive oxygen species (ROS) generation, thereby increasing HIF-1α expression, which is critical for eliciting CIH-induced cardiorespiratory responses by the CB. CIH also increases ROS generation and TH expression in the AM, although it is less sensitive than the CB (10).

Recent studies have identified that IPAS, which is one of the alternatively spliced variants of HIF-3α, acts as a dominant negative inhibitor of HIF-1α by a direct interaction with HIF-1α and prevents its DNA binding (11). IPAS is predominantly expressed in the Purkinje cells of the cerebellum and corneal epithelium. In addition, because the IPAS gene has an HRE sequence in its promoter, IPAS can be induced by hypoxia in the heart and lung. Therefore, IPAS acts as a negative feedback inhibitor of HIF-1α (12).

Magnesium deficiency is believed to be related to many diseases, such as hypertension, ischemic heart disease, and diabetes mellitus (13–16). However, the molecular mechanisms underlying the role of magnesium in the pathogenesis of these diseases have been largely undefined. Our analyses here demonstrate that magnesium deficiency causes a loss of ROS-induced HIF-1α activity by inducing IPAS gene expression.

EXPERIMENTAL PROCEDURES

Cell Culture, DNA Transfection, and IH Treatment—PC12, Hep3B, C6, and B16-f10 cells were obtained from the Cell Resource Center for Biomedical Research of Tohoku University. PC12 cells were maintained in RPMI 1640 (Wako Pure Chemical Industries) supplemented with 10% fetal bovine serum in collagen IV-coated dishes (BD Biosciences) under 5% CO_2 at 37 °C and transferred every 3 days. Transfection was performed using the lipofection reagent (TransFast; Promega)

[2] The abbreviations used are: HIF, hypoxia-inducible factor; ROS, reactive oxygen species; TH, tyrosine hydroxylase; HRE, hypoxia response element; AM, adrenal medulla; CB, carotid body; IH, intermittent hypoxia; CIH, chronic IH; OSA, obstructive sleep apnea; PAS, Per/Arnt/Sim; IPAS, inhibitory PAS domain protein; DMEM, Dulbecco's modified Eagle's medium; PMA, phorbol 12-myristate 13-acetate; NAC, N-acetyl-L-cysteine; RT, reverse transcription; siRNA, small interfering RNA; PI3K, phosphatidylinositol 3-kinase; PKC, protein kinase C.

according to the manufacturer's protocol. The change of RPMI to DMEM (Wako Pure Chemical Industries) was performed 1 day before transfection experiments, and cells were transfected in serum-free DMEM. After the cells were incubated for 1 h, each appropriate medium was added, and the cells were treated with 100 μM cobalt chloride ($CoCl_2$) for 10 h. The growth rate of PC12 cells in the two media was similar (data not shown). IH treatment was carried out as follows. 1.5 h after transfection, the cells were exposed to 54 cycles of 15 s in duration at 4.5% O_2 followed by 2 min at 21% O_2, approximately seven episodes/h, 8 h/day with 10% CO_2 in an O_2/CO_2 incubator (Wakenyaku, Co., Ltd). The cells exposed to room air with 10% CO_2 (normoxia) in a CO_2 incubator served as controls. Hep3B, B16-f10, and C6 cells were grown in DMEM, RPMI, and RPMI, respectively, with 10% fetal bovine serum. Hep3B and C6 cells were transfected by the calcium-phosphate precipitation method. B16-f10 cells were transfected by Lipofectamine 2000 (Invitrogen). Construction of the HRE-dependent luciferase reporter plasmid and the assay of luciferase activity were described previously (17). Data from PC12 and B16-f10 cells were normalized to the concentration of protein. E1b-luciferase 2 (E1b-luc2) with five copies of NF-κB response element plasmid (NF-κB REx5-E1b-luc2) was constructed by inserting five copies of the sequence (5'-GGGAATTTCC-3') between the BglII site and NheI of the E1b-luc2 plasmid. The dual luciferase reporter assay was performed according to the manufacturer's protocol (Promega).

Drug Treatments—Drugs were purchased as follows: MK-801, nifedipine, sulfasalazine, NF-κB SN50 cell-permeable inhibitor peptide, cyclosporin A, and rottlerin were from Calbiochem; NAC, mibefradil, BMS-345541, and PMA were from Sigma-Aldrich; LY294002 was from Cell Signaling Technology; cilnidipine was from BIOMOL International LP; and A23187 was from Wako Pure Chemical Industries. The cells were treated with each drug 30 min before 100 μM $CoCl_2$ treatment.

Measuring Calcium Concentration—Calcium levels in the cells were determined using the fluorescent probe Fluo-8 AM (ABD Bioquest, Inc.). PC12 cells were cultured in a collagen IV-coated 35-mm glass-bottomed dish. The growth medium was removed, and the cells were incubated with 2.5 μM Fluo-8 AM, 10% Pluronic F-127 (ABD Bioquest, Inc.), 250 mM probenecid (Invitrogen), and 20 mM Hepes in Hanks' balanced salt solution (Invitrogen) at 37 °C, 5% CO_2 incubator for 30 min. The cells were washed with phosphate-buffered saline and then incubated in serum-free, phenol red-free DMEM or RPMI for 30 min with 50 ng/ml Hoechst 33342. After incubation, the cells were treated with $CoCl_2$ for 5 min and imaged with a fluorescence microscope (Olympus IX71). PC12 cells were treated with 8 μg/ml A23187 as controls.

Animals—Male C57BL/6J Jms Slc mice ($\sim$16 weeks of age) were randomly divided into two groups, with each group having a similar mean body weight, and fed on a magnesium-deficient diet (AIN-93 M diet, Low-Mg, Nihon Nosan Kogyo Co., Japan) or a normal diet (AIN-93 M diet, standard) for 14 days in a 12-h light and 12-h dark cycle at 23 °C. The magnesium-deficient diet and the normal diet contained 0.0004% and 0.0844% magnesium, respectively. A dose of 60 μg of $CoCl_2 \cdot 6H_2O$ or saline/g

of body weight was administered intraperitoneally. In the case of CIH, the mice were randomly divided into two groups; the mice in each group had similar mean body weights, but one group was fed on the magnesium-deficient diet, whereas the other had been fed on the normal diet for 3 weeks. The mice were exposed to CIH (54 cycles consisting of 15 s at 6% O_2 followed by 5 min at 21% O_2, approximately seven episodes/h, 8 h/day) for the last 2 weeks in the O_2/CO_2 incubator (Wakenyaku, Co., Ltd). Mice exposed to room air of 21% O_2 (normoxia) served as controls. Serum magnesium levels were determined colorimetrically using the Wako Magnesium B test kit (Wako Pure Chemical Industries). Animal care and use were reviewed and approved by the Committee for Animal Research of Tohoku University.

Western Blotting—Nuclear extracts or cell lysate were prepared from PC12 cells and Hep3B cells as described previously (17). The proteins were extracted from the adrenal gland using the extraction reagent (T-PER; Pierce). A total of 35 μg (from cells) or 15 μg (from mice) of protein was loaded on an 8% SDS-polyacrylamide gel. HIF-1α, TH, and IκB-α were detected using the ECL Western kit (GE Healthcare). The anti-TH antibody was a generous gift from Dr. I. Nagatsu. The anti-HIF-1α monoclonal antibody and an anti-IκB-α monoclonal antibody were purchased from Novus Biologicals and Cell Signaling Technology, respectively.

RT-PCR—Total RNA was extracted from cultured cells or adrenal glands using RNA isolating reagent (RNAiso; Takara Bio). cDNAs were synthesized using oligonucleotide random hexamers (Takara Bio) and Moloney murine leukemia virus reverse transcriptase (Invitrogen). A fraction (1 μl) of synthesized cDNA was amplified in a 20-μl reaction mixture containing 5 units of Taq polymerase (Ex TaqHS; Takara Bio). PCR cycles were chosen within the linear range of amplification. The PCR procedure consisted of 20 cycles of reaction for 18 S rRNA cDNA, 21 for β-actin, 21 for TH, 28 for HIF-1α-like factor, 30 for HIF-1α, 33 for HIF-3α, 35 for VHL and IPAS: 94 °C for 30 s, 60 °C for 30 s, and 72 °C for 30 s. The bands were quantified by using Image J software. For amplification of mouse IPAS, we employed 33 cycles of reaction: 96 °C for 15 s and 68 °C for 1 min using KOD-Plus-polymerase (Toyobo), and the PCR products were electrophoresed on 6% polyacrylamide gels and quantified on an Imaging analyzer (Fuji BAS1000). The primers used for the reaction are described in supplemental Table S2. For rat IPAS primers, the rat IPAS putative exon 16 sequence was found by homology search in the NCBI data base.

siRNA—RNA oligonucleotides (21 nucleotides) homologous to HIF-3α/IPAS were designed as follows: forward, 5'-GCUCA UUGGA CACAG UAUCT T, and reverse, 5'-GAUAC UGUGU CCAAU GAGCT T; and control siRNA homologous to green fluorescent protein sequence, forward, 5'-GGCUA CGUCC AGGAG CGCAT T, and reverse, 5'-UGCGC UCCUG GACGU AGCCT T. The cells were treated with annealed siRNAs using Oligofectamine (Invitrogen) according to the manufacturer's protocol. After 24 h, the change of RPMI to DMEM was carried out. Subsequent transfection was performed as described above.
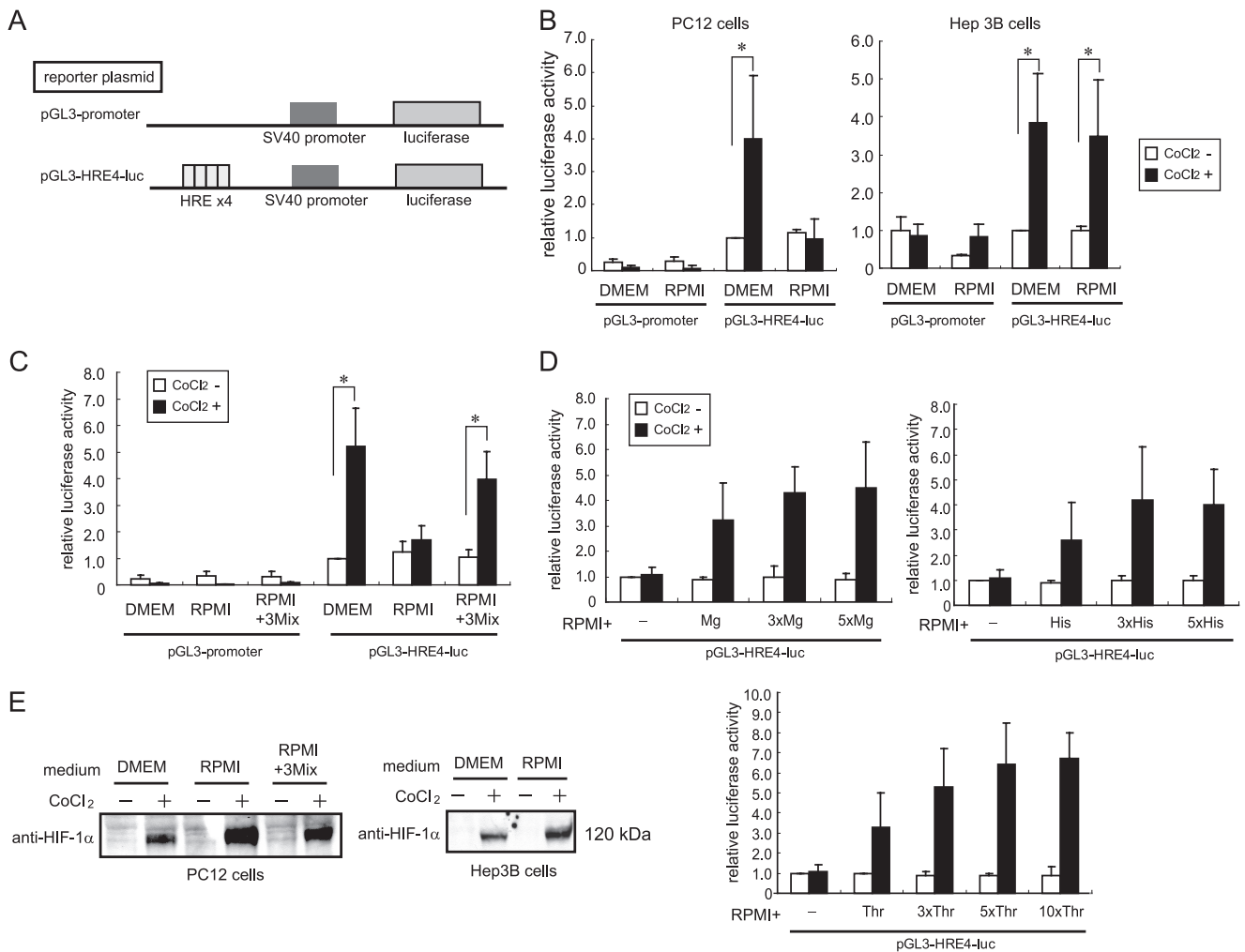
FIGURE 1. **Loss of hypoxic response induced by CoCl₂ in RPMI-cultured PC12 cells.** *A*, schematic representation of reporter plasmids. *B*, medium-dependent induction of reporter activity induced by CoCl₂ in PC12 cells. *C*, chemical hypoxia-inducible reporter activity recovered by the addition of magnesium, Thr, and His to RPMI. *3Mix* indicates a mixture of magnesium, Thr, and His, giving equivalent concentrations to those present in DMEM. *D*, effect of addition of increasing amounts of magnesium, His, and Thr to RPMI on reporter activity. *1x*, *3x*, *5x*, and *10x* indicate addition of amino acids to RPMI whose concentrations are equal to, three times, five times, and 10 times higher than that of DMEM. *E*, Western blot analysis of HIF-1α protein induced by CoCl₂ in PC12 and Hep3B cells. *, $p < 0.05$ for indicated comparison. The data shown in the bar graphs are the averages ± S.D. of three independent experiments.

In Situ Hybridization—The adrenal gland and CB were fixed in neutral buffered formalin (Mildform10N; Wako Pure Chemical Industries) at 4 °C overnight, dehydrated in an ethanol series, embedded in paraffin, and cut into 8-μm sections. Tissue sections were deparaffinized in xylene and rehydrated in a graded series of ethanol. Subsequently, sections of the adrenal gland and CB were treated with 1 μg/ml proteinase K (Roche Applied Science) in phosphate-buffered saline at room temperature for 12 and 5 min, respectively, and the sections of the adrenal gland were acetylated. Hybridization was carried out in a solution containing 50% formamide, 2× SSC, 1 μg/μl tRNA, 1 μg/μl salmon sperm DNA, 1 μg/μl bovine serum albumin, 10% dextran sulfate, and digoxigenin-linked cRNA probes for 18 h at 55 °C. Digoxigenin-linked cRNA probes for TH mRNA (nucleotides 1139–1525) were synthesized by T7 (antisense) or T3 (sense) RNA polymerase using a pBlueScript SK(+)-based template. The samples were treated with an anti-digoxigenin antibody conjugated with alkaline phosphate (Roche

Applied Science) in 1:100 dilution for 30 min at room temperature and subsequently reacted with 330 μg/ml NBT, 165 μg/ml 5-bromo-4-chloro-3-indolyl phosphate, and 1 mM levamisole for 18 h at room temperature. It was counterstained with the nuclear dye, kernechtrot (red) (Muto Pure Chemicals).

Immunohistochemistry—The samples were prepared similarly as mentioned above. All of the sections were treated for 30 min with 3% hydrogen peroxide in methanol to quench endogenous peroxidase activity. An antibody against TH was used as the first antibody in dilution 1:100,000. A secondary antibody reaction was carried out using horseradish peroxidase-linked anti-rabbit goat IgG at room temperature for 1 h. The samples were subsequently reacted with 3,3′-diaminobenzidine and counterstained with the nuclear dye, kernechtrot (red) or hematoxylin (dark blue).

Statistical Analysis—The data are given as the means ± standard deviation, with the number of the experiments indicated. Statistical significance was established by paired Stu-
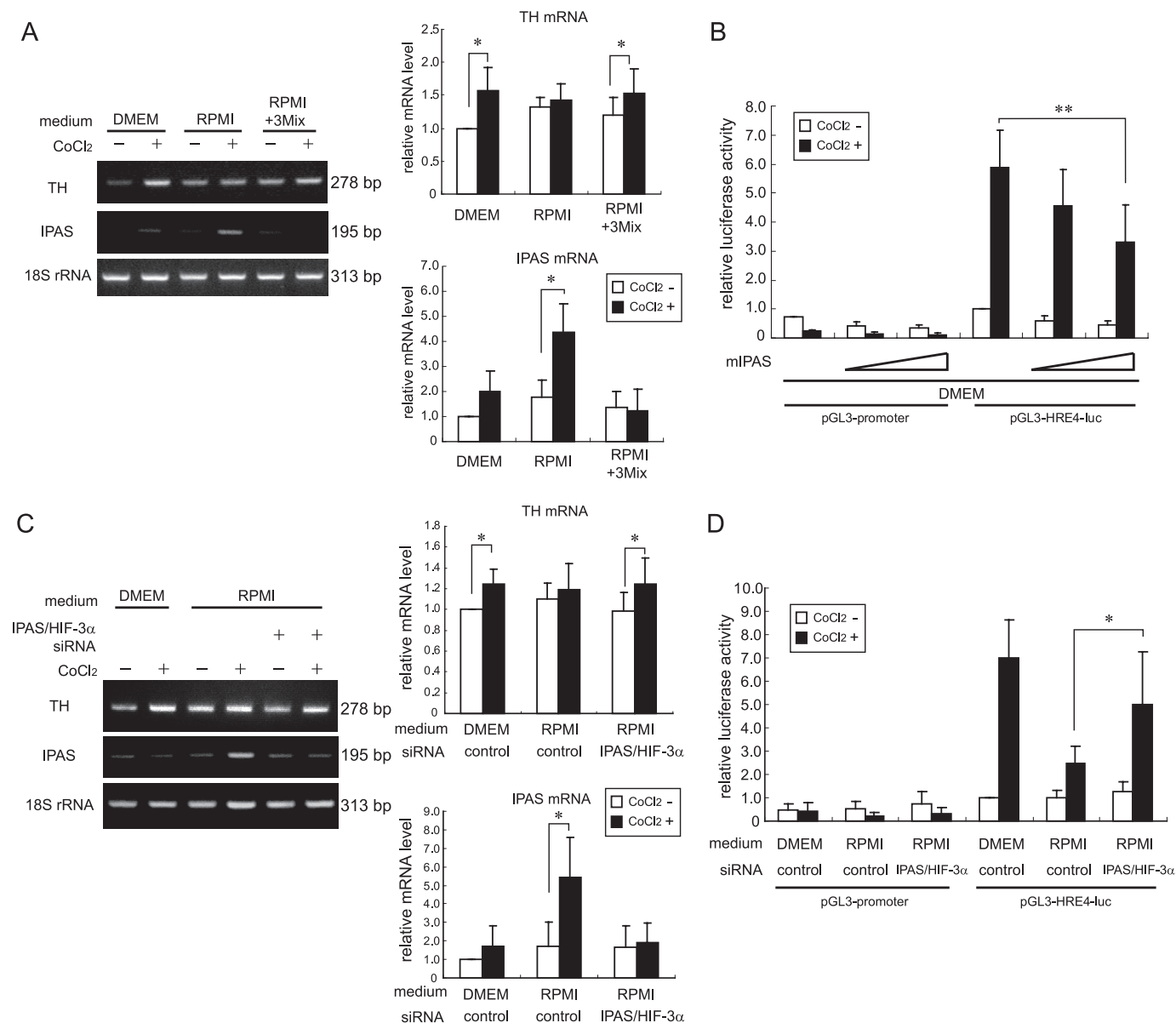
FIGURE 2. **IPAS is responsible for suppression of the hypoxic response.** *A*, TH and IPAS gene expression in CoCl₂-treated PC12 cells cultured in different media. mRNA expression levels were determined by RT-PCR. PCR products were analyzed on 2% agarose gels (*left panel*) and quantified by densitometry. The data were normalized to 18 S rRNA, and the value of cells cultured in DMEM without CoCl₂ was set to 1. *B*, repression of HRE-dependent luciferase activity by coexpression of IPAS. mIPAS indicates the mouse IPAS expression plasmid. PC12 cells in 6-well plates were transfected with mIPAS (0.45 μg or 0.9 μg). *C*, inducible expression of TH mRNA recovered by treatment with IPAS/HIF-3α siRNA in RPMI-cultured PC12 cells. mRNA expression levels were determined by RT-PCR. *D*, inducible expression of reporter activity recovered by the treatment with IPAS/HIF3α siRNA. Green fluorescent protein siRNA was used for control. *, $p < 0.05$ for indicated comparison. **, $p < 0.01$ for indicated comparison. The data shown in the bar graphs are the averages ± S.D. of four independent experiments.

dent's *t* tests. In experiments using the adrenal gland (see Fig. 4, *B* and *D*), statistical significance was established by unpaired Student's *t* tests.

RESULTS

Loss of Hypoxic Response Induced by CoCl₂ in RPMI-cultured PC12 Cells—To examine the hypoxic response of PC12 cells in different nutritional conditions, we introduced a reporter plasmid containing HREs (Fig. 1*A*) (17) and treated with CoCl₂, a chemical mimetic of hypoxia. In DMEM-cultured PC12 cells, a 4-fold induction of reporter activity was found in response to CoCl₂ (Fig. 1*B*). However, in the RPMI 1640 medium (RPMI), no increase in luciferase activity was observed (Fig.

1*B*). When human hepatoma Hep3B cells, mouse melanoma B16-F10 cells and rat glioma C6 cells were used, the hypoxic response was observed in both DMEM and RPMI (Fig. 1*B* and supplemental Fig. S1), indicating that the medium dependence was cell type-specific. We attempted to identify the causal nutrients for the loss of HIF transactivation activity. Medium-specific nutrients were examined, but they exhibited no effect on the distinct hypoxic response (supplemental Fig. S1 and supplemental Table S1, groups 1 and 6). Because almost all the common nutrients included were richer in DMEM than in RPMI, we divided the nutrients into four groups (supplemental Table S1, groups 2–5), added
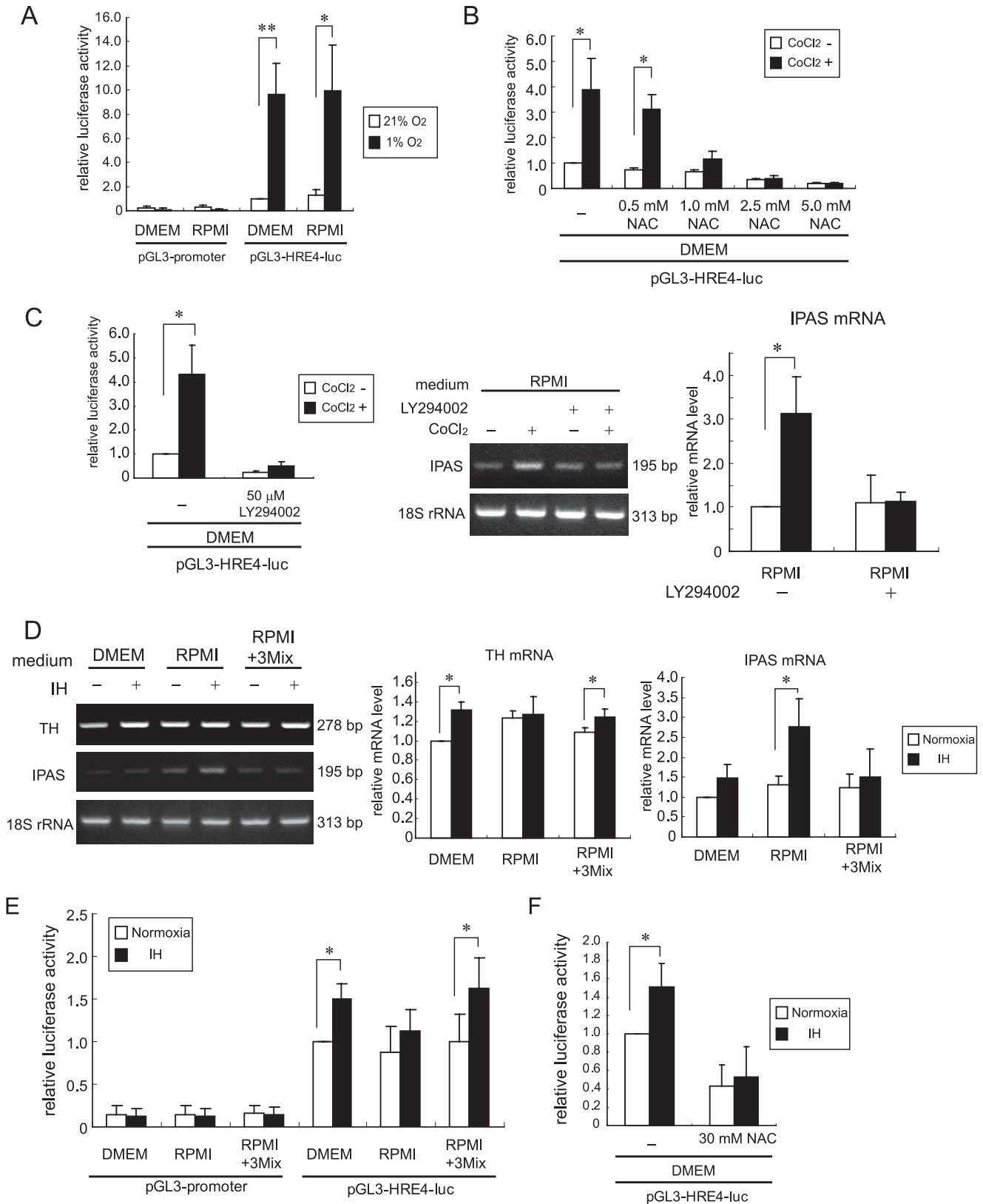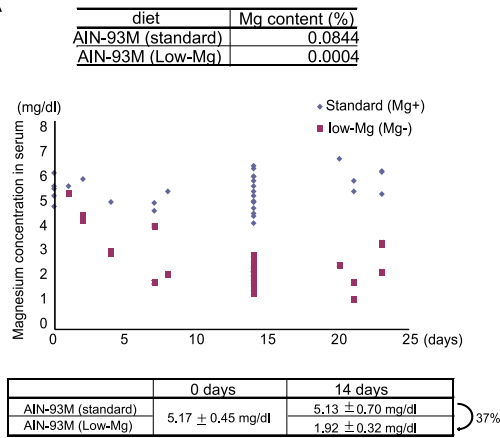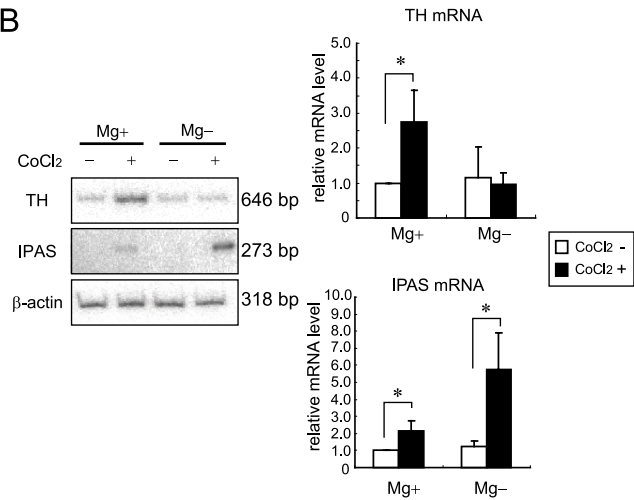
FIGURE 3. **Activation of the ROS-PI3K pathway by CoCl$_2$ and intermittent hypoxia in PC12 cells.** *A*, expression of reporter activity induced by sustained hypoxia in PC12 cells. *B*, inhibition of CoCl$_2$-induced luciferase activity by NAC. *C*, LY294002 (50 μM) inhibited CoCl$_2$-induced HIF-1α activity (*left panel*) and the induction of IPAS mRNA in RPMI (*right panel*). *D*, TH and IPAS gene expression in PC12 cells exposed to IH in different culture media. *3Mix* indicates a mixture of magnesium, His, and Thr as mentioned in Fig. 1*C*. *E*, expression of reporter activity in PC12 cells exposed to IH in different culture media. *F*, inhibition of reporter activity by NAC in PC12 cells exposed to IH. *, $p < 0.05$ for indicated comparison. **, $p < 0.01$ for indicated comparison. The data shown in the bar graphs are the averages ± S.D. of three independent experiments.

A

diet	Mg content (%)
AIN-93M (standard)	0.0844
AIN-93M (Low-Mg)	0.0004

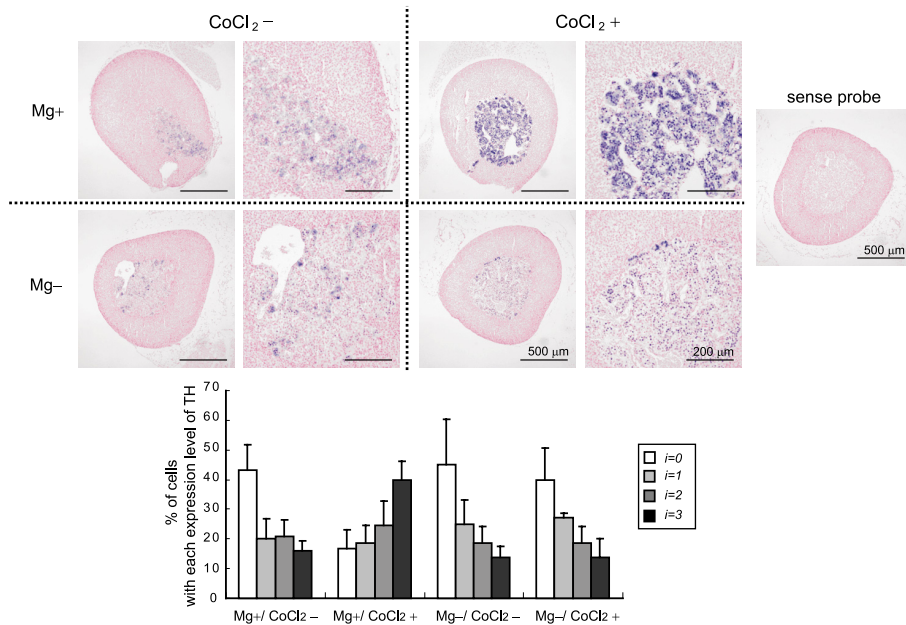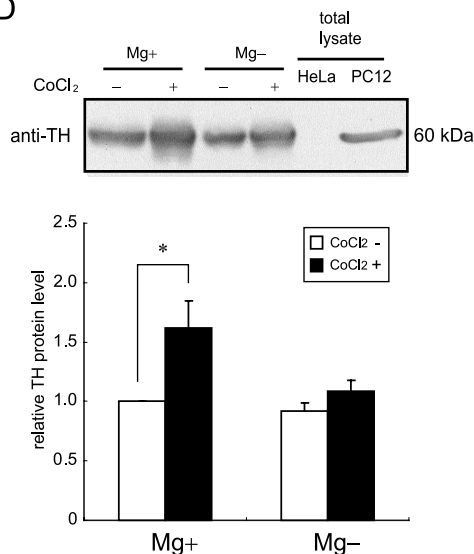|	0 days	14 days	
AIN-93M (standard)		5.13 ± 0.70 mg/dl	
AIN-93M (Low-Mg)	5.17 ± 0.45 mg/dl	1.92 ± 0.32 mg/dl	37%

B
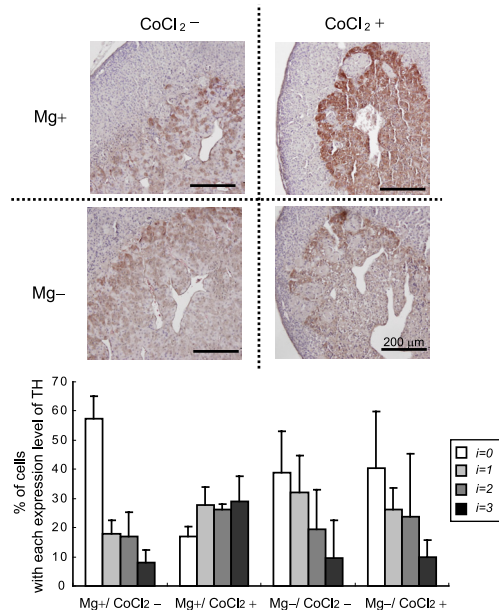

C

D

E

excess amounts of grouped nutrients to RPMI and assayed the reporter activity (supplemental Fig. S1). Subsequently, each nutrient in the positive groups was tested (supplemental Fig. S1). Consequently, three nutrients, magnesium, histidine, and threonine, were identified. In PC12 cells cultured in RPMI that contained these three nutrients at concentrations equivalent to those in DMEM, the $CoCl_2$-induced hypoxic response was recovered (Fig. 1*C*). The addition of each nutrient to RPMI yielded hypoxic responsibility in a dose-dependent manner (Fig. 1*D*). We examined the possibility that HIF-1α protein stability was decreased in RPMI-cultured PC12 cells. However, the nuclear HIF-1α protein was stabilized by the treatment of $CoCl_2$ in both DMEM and RPMI media (Fig. 1*E*). The addition of the three nutrients to RPMI had no effect on the stabilization of HIF-1α.

IPAS Is Responsible for Suppression of Hypoxic Response— We investigated the possibility that IPAS is involved in the nutrient-dependent hypoxic response. As expected, IPAS mRNA was significantly induced in response to $CoCl_2$ only when PC12 cells were cultured in RPMI (Fig. 2*A*). The addition of a mixture of magnesium, His, and Thr to RPMI inhibited the induction of IPAS mRNA, and the inducible expression of the TH gene was recovered (Fig. 2*A*). The expression levels of HIF-1α, HIF-1α-like factor (also known as HIF-2α or EPAS1), and VHL mRNAs remained unchanged in PC12 cells regardless of the culture media and whether they were treated with $CoCl_2$ (supplemental Fig. S2). HIF-3α mRNA was very weakly expressed in PC12 cells cultured in both media and was apparently not affected by the presence of $CoCl_2$. The overexpression of IPAS apparently inhibited HRE-dependent reporter activity, although its inhibition was incomplete even when large amounts of the IPAS expression plasmid were used (Fig. 2*B*). The endogenous IPAS mRNA level was decreased by IPAS/HIF-3α siRNA treatment (Fig. 2*C*). The siRNA treatment recovered the induction of TH mRNA by $CoCl_2$ in RPMI-cultured PC12 cells. Furthermore, induction of reporter activity was also recovered to some extent by the suppression of IPAS expression (Fig. 2*D*). HIF-3α mRNA was very weakly expressed, and we were unable to detect a down-regulation of the expression by the treatment (supplemental Fig. S2).

Activation of the ROS-PI3K Pathway by $CoCl_2$ and Intermittent Hypoxia in PC12 Cells— We examined whether the loss of HIF activity in RPMI is observed when PC12 cells were treated by sustained hypoxia. The inducible expression of luciferase activity was caused by hypoxia in both DMEM and RPMI (Fig. 3*A*), suggesting different mechanisms leading to hypoxic response of the cells between hypoxia and $CoCl_2$. To examine whether the ROS-

phosphatidylinositol 3-kinase (PI3K) pathway is involved in the induction of HIF-1α by $CoCl_2$, we used a ROS scavenger, NAC, and a PI3K inhibitor, LY294002. When treated with NAC, the up-regulation of luciferase activity was impaired in a dose-dependent manner (Fig. 3*B*). Moreover, $CoCl_2$ failed to induce HIF-1α activity in DMEM and IPAS mRNA in RPMI when treated with LY294002 (Fig. 3*C*). These results suggest that HIF-1α is induced by $CoCl_2$ via the ROS-PI3K pathway.

To examine the cellular response to IH, PC12 cells were exposed either to 21% O_2 (normoxia) or to 54 cycles of IH. TH mRNA was weakly but reproducibly induced by IH in PC12 cells cultured in DMEM, but not in RPMI (Fig. 3*D* and supplemental Fig. S3). The addition of the three nutrients to RPMI recovered the inducibility of TH mRNA. IPAS mRNA was induced only in RPMI-cultured PC12 cells in response to IH. Moreover, an approximate 1.5-fold induction of luciferase activity was found in DMEM-cultured PC12 cells in response to IH (Fig. 3*E*). On the other hand, the induction was modest in the cells grown in RPMI but was recovered when the three nutrients were added to RPMI. Furthermore, inducible luciferase activity in DMEM caused by IH was inhibited by NAC (Fig. 3*F*). Collectively, these results demonstrate that the induction of HIF-1α activity by IH as well as $CoCl_2$ is ROS-dependent and suggest that IPAS induced by IH is responsible for the inhibition of the ROS-mediated HIF-1α activity.

Hypomagnesemia Suppresses Response to $CoCl_2$ and CIH in the AM and CB— We hypothesized that suppression of the hypoxic response caused by a deficiency of the nutrients might also occur *in vivo*. We focused on magnesium as a deficient nutrient because magnesium deficiency is known to be involved in many age-related diseases, and its serum level is relatively easily controlled by diet. Because PC12 cells were derived from the AM, the hypoxic response in the AM of mice with hypomagnesemia was investigated. Fig. 4*A* shows that serum magnesium levels were gradually decreased in mice fed on a magnesium-deficient diet. In 2 weeks, serum magnesium levels of mice fed on a magnesium-deficient diet were decreased to ~40% of control mice, and they were used for analysis of hypoxia-related gene expression by RT-PCR. TH mRNA was induced in the adrenal gland of normal mice by the injection of $CoCl_2$, but not in magnesium-deficient mice (Fig. 4*B*). IPAS mRNA was weakly (2.0-fold) induced in normal mice by the injection of $CoCl_2$. In contrast, a strong induction (6.0-fold) was observed in $CoCl_2$-injected magnesium-deficient mice. HIF-1α, HIF-1α-like factor, and HIF-3α mRNAs were relatively evenly expressed in the mice regardless of their diets or whether they had been injected with $CoCl_2$ (supplemental

FIGURE 4. **Hypomagnesemia suppresses response to $CoCl_2$ in the AM.** *A*, change in the serum magnesium level of mice fed on a normal or magnesium-deficient diet. The average serum magnesium concentrations at 0 and 14 days in magnesium-deficient and normal mice are shown below. *B*, TH and IPAS gene expression in the adrenal gland of magnesium-deficient mice induced by $CoCl_2$ injection. The mice were dissected at 6 h after $CoCl_2$ administration. The relative levels of mRNA in the adrenal gland were determined by RT-PCR analysis and normalized to β-actin mRNA. *C*, *in situ* hybridization analysis of TH expression (*blue*) in the adrenal gland of $CoCl_2$-injected magnesium-deficient mice. The sections were counterstained with the nuclear dye, kernechtrot (*red*). Higher magnification images are also shown. The cells were divided into four groups ($i = 0$–3) in terms of TH mRNA levels, negative or very weak ($i = 0$), weak ($i = 1$), intermediate ($i = 2$), and strong ($i = 3$), and cells with respective expression levels were scored. *D*, immunoblot analysis for TH expression in the adrenal gland of $CoCl_2$-injected magnesium-deficient mice. The mice were dissected at 24 h after $CoCl_2$ administration. Cell extracts of HeLa and PC12 cells were used as negative and positive controls, respectively. Quantified results by densitometry are also shown. *E*, immunohistological analysis of TH protein (*brown*) in the adrenal gland of $CoCl_2$-injected mice. The sections were counterstained with the nuclear dye, hematoxylin (*dark blue*). The cells were divided into four groups and scored as shown in *C*. *, $p < 0.05$ for indicated comparison. The data shown in the bar graphs are the averages ± S.D. of three independent experiments.
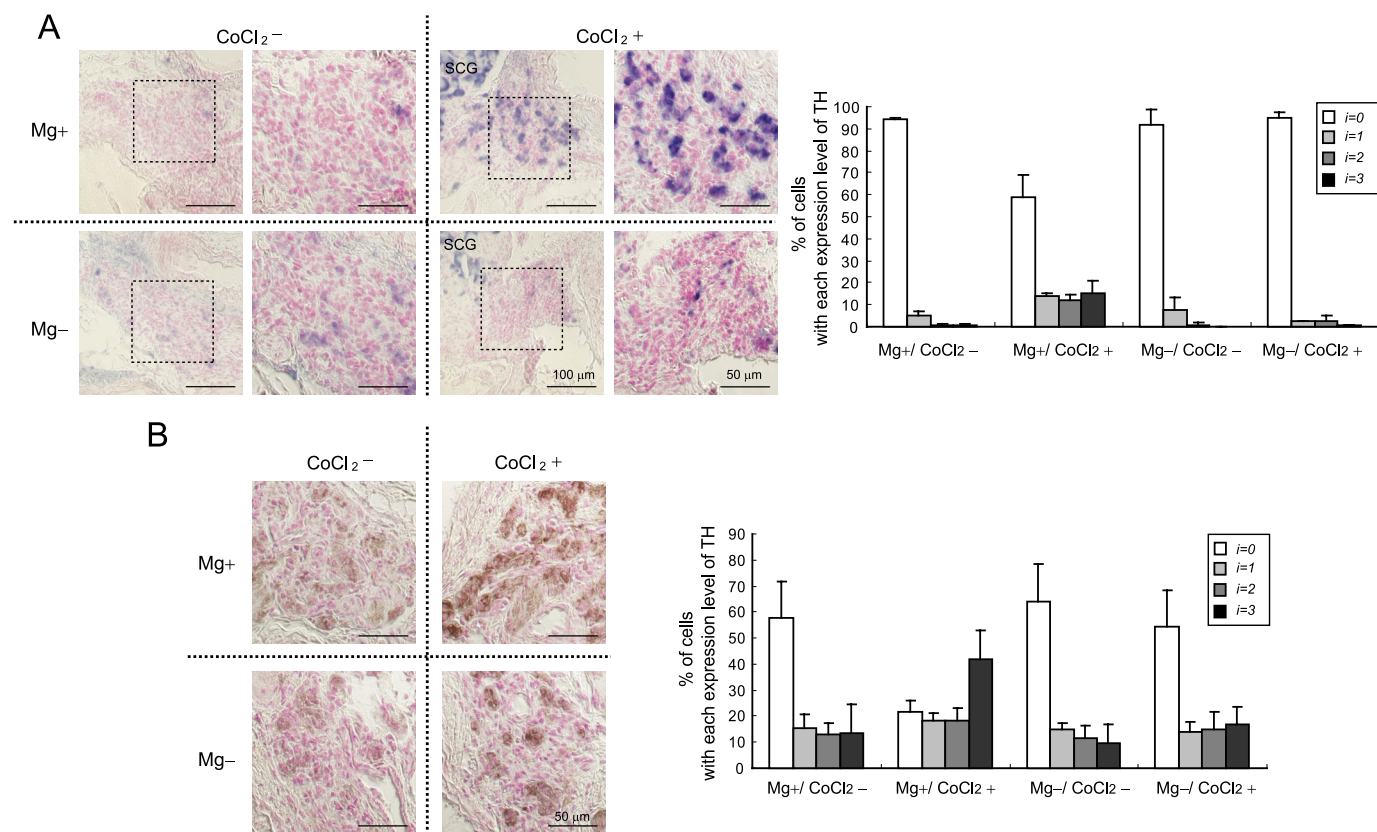
FIGURE 5. **Hypomagnesemia suppresses response to CoCl₂ in the CB.** *A*, *in situ* hybridization of TH expression in the CB of CoCl₂-injected magnesium-deficient mice. The mice were dissected at 24 h after CoCl₂ administration. The sections were counterstained with kernechtrot. CBs with higher magnification images are also shown (*rectangle area*). The cells were divided into four groups ($i = 0$–3) in terms of TH expression levels as shown in Fig. 4C, and cells with respective expression levels were scored. TH mRNA was constitutively expressed in neurons of the superior cervical ganglion regardless of CoCl₂ treatment. *B*, immunohistochemical analysis of TH expression in the CB of CoCl₂-injected magnesium-deficient mice. The cells were divided into four groups as shown in Fig. 4C. The data shown in the bar graphs are the averages $\pm$ S.D. of three independent experiments.

Fig. S4). Moreover, *in situ* hybridization experiments showed that TH mRNA was induced in the AM of CoCl₂-injected normal mice but not at all in magnesium-deficient mice (Fig. 4C). Western blotting (Fig. 4D) and immunostaining assays (Fig. 4E) have shown that TH protein was up-regulated in normal mice but not in magnesium-deficient mice by CoCl₂ injection.

We investigated the hypoxic response of CB in mice with magnesium deficiency. *In situ* hybridization assays showed that TH expression in the CB was increased in CoCl₂-injected normal mice but not in magnesium-deficient mice (Fig. 5A). Immunostaining assays also showed that TH protein levels in the CB were enhanced in CoCl₂-injected normal mice but not in magnesium-deficient mice (Fig. 5B).

We next examined whether the loss of TH up-regulation is observed in magnesium-deficient mice exposed to CIH (Fig. 6A). As expected, *in situ* hybridization experiments (Fig. 6B) and immunostaining assays (Fig. 6C) clearly showed that both TH mRNA and protein were increased in CIH-exposed normal mice but not at all in magnesium-deficient mice. The response to CIH in the adrenal gland was also investigated. However, TH in the AM was not induced in normal mice under the CIH conditions used in this study,[3] confirming previous results that

the AM is less sensitive to CIH than the CB (10). Further extensive exposure of mice to CIH is necessary to clarify the inducibility of TH expression in the AM.

Molecular Mechanism Leading to IPAS Gene Activation—We investigated the mechanism that results in activation of the IPAS gene in PC12 cells. Because magnesium acts as a calcium antagonist at multiple voltage-gated channels (18), their involvement was investigated. As shown in Fig. 7A, an increase in the intracellular calcium level was observed 5 min after CoCl₂ treatment of PC12 cells cultured in RPMI but not in DMEM. A pharmacological calcium channel blocker, mibefradil, which inhibits T-type channels and also weakly inhibits L-type channels (19), inhibited the induction of IPAS mRNA and activated reporter activity in response to CoCl₂ (Fig. 7B). NiCl₂, which is a specific inhibitor of the T-type calcium channels (20) and also a chemical mimetic of hypoxia like CoCl₂ (2), inhibited the activation of the IPAS gene and activated reporter activity in RPMI-cultured PC12 cells (Fig. 7C). The addition of MK-801, an *N*-methyl-D-aspartate receptor antagonist, weakly activated the reporter activity in response to CoCl₂ (Fig. 7D). Nifedipine and cilnidipine, L-type channel-specific and both L-type and N-type channel-specific blockers, respectively, were of no effect.[3] Treatment of cells with calcium ionophore, A23187, induced expression of IPAS mRNA in response to CoCl₂ treatment and inactivated HRE-dependent reporter

---

[3] S. Torii, K. Kobayashi, M. Takahashi, K. Katahira, K. Goryo, N. Matsushita, K.-I. Yasumoto, Y. Fujii-Kuriyama, and K. Sogawa, unpublished data.
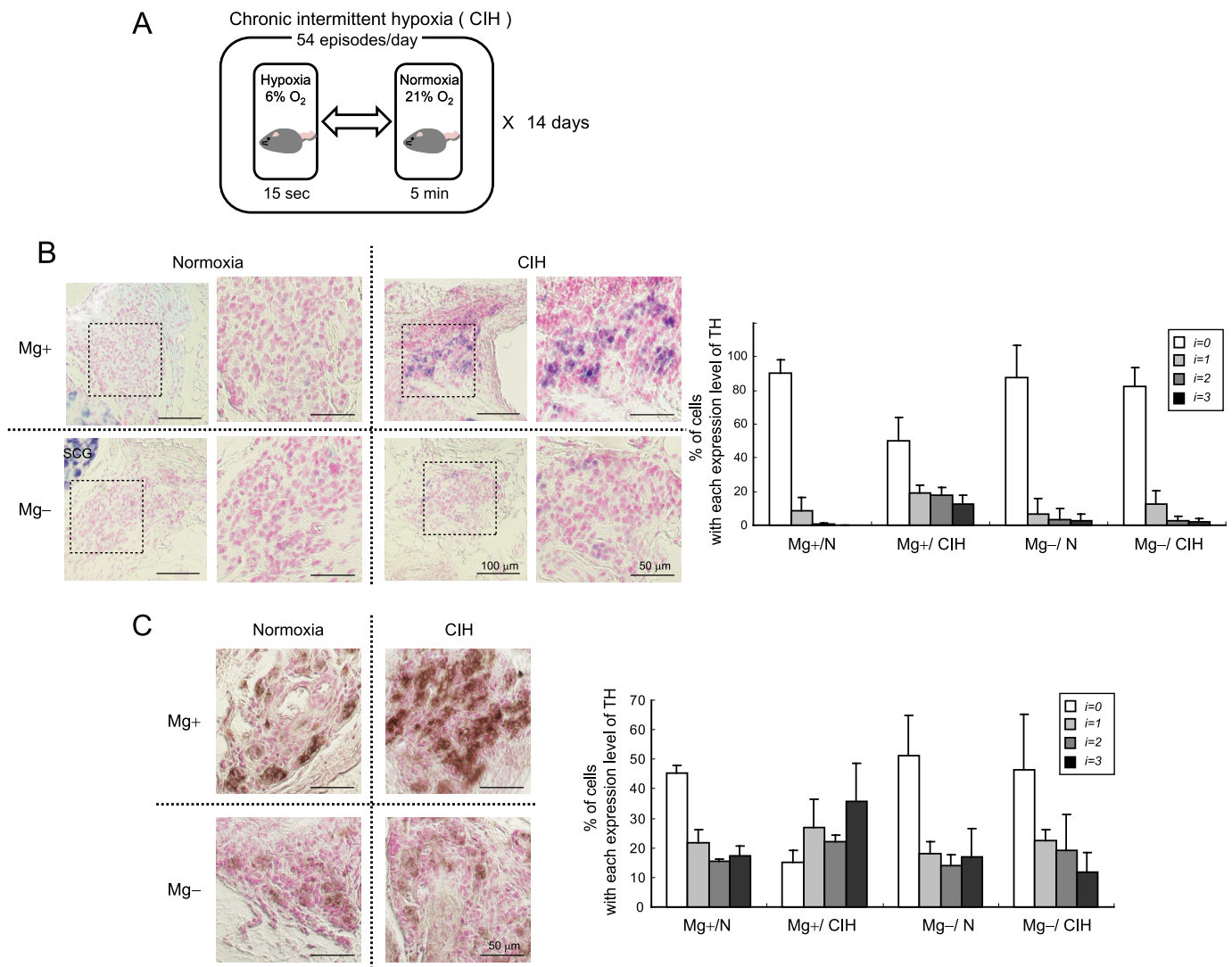
FIGURE 6. **Hypomagnesemia suppresses response to CIH in the CB.** *A*, experimental protocol for CIH. The mice were fed on a normal or magnesium-deficient diet for 3 weeks and exposed to CIH in the last 2 weeks. *B*, *in situ* hybridization of TH expression in the CB of magnesium-deficient mice exposed to CIH. CBs with higher magnification images are also shown (*rectangle area*). The cells were divided into four groups ($i = 0$–3) in terms of TH expression levels as shown in Fig. 4*C*, and cells with respective expression levels were scored. *C*, immunohistochemical analysis of TH expression in the CB of magnesium-deficient mice exposed to CIH. The cells were divided into four groups as shown in Fig. 4*C*. The data shown in the bar graphs are the averages ± S.D. of three independent experiments.

activity (Fig. 7*E*). These results suggest that calcium influx mainly through the T-type calcium channels is involved in the ROS-dependent IPAS gene expression in PC12 cells cultured in RPMI.

An increase in intracellular calcium levels possibly activates several transcription factors such as NF-κB, CREB, and NFAT. We tested several inhibitors for the canonical NF-κB pathway. Sulfasalazine (an IKK inhibitor) and BMS-345541 (a specific inhibitor of IKKβ and weak inhibitor of IKKα) blocked induction of IPAS and enhanced reporter activity in response to CoCl$_2$ in RPMI (Fig. 8*A*). SN50, a peptide inhibitor for nuclear translocation of NF-κB, also inhibited IPAS expression and activated reporter activity (Fig. 8*A*). There was also a weak decrease of IκB-α at 15 min after CoCl$_2$ treatment in RPMI-cultured PC12 cells (Fig. 8*B*). NF-κB-dependent reporter activity in the RPMI-cultured PC12 cells was induced by CoCl$_2$ (Fig. 8*B*). These results indicate that increased calcium levels result

in activation of NF-κB. PMA, an activator of conventional and novel PKC isotypes (21), inhibited induction of HRE reporter activity, and enhanced IPAS expression regardless of CoCl$_2$ treatment (Fig. 8*C*). An activator of CREB, dibutyryl cAMP, was of no effect, and a CRE reporter was not activated by CoCl$_2$.[3] Cyclosporin A, inhibitor of calcineurin, which is a protein phosphatase and activates NFAT, activated neither IPAS gene expression nor HRE-dependent reporter activity in response to CoCl$_2$ in RPMI (supplemental Fig. S5).

DISCUSSION

Previous studies have shown that HIF-1α in normoxia is hydroxylated by prolyl hydroxylases in an O$_2$ and Fe^{2+}-dependent manner and recognized by pVHL, leading to degradation. It is therefore generally accepted that prolyl hydroxylase activity is inhibited by sustained hypoxia and by Co^{2+} that can substitute active-site Fe^{2+} (22). However, recent
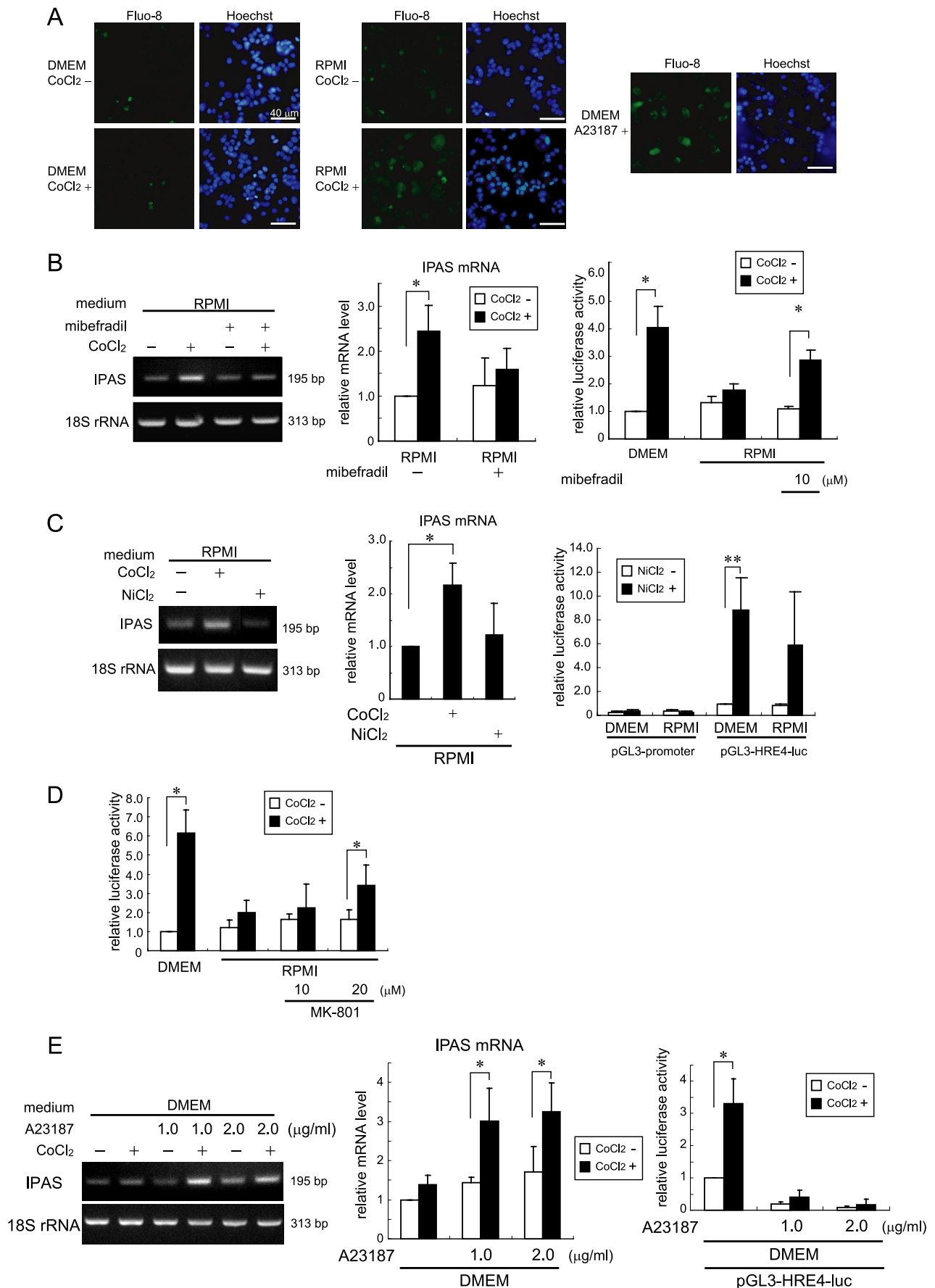
reports have shown that the induction of HIF-1α by CoCl$_2$ is dependent on ROS and PI3K signaling-mediated protein translation (23, 24). CoCl$_2$ activates the PI3K pathway by ROS generation, and PI3K-Akt enhances the translation of cellular mRNAs, including HIF-1α mRNA. The results from a present study are in good accordance with the conclusion from the latter studies that CoCl$_2$ acts as a ROS generator, leading to activation of PI3K.

In human, ROS-dependent hypoxic response is caused by OSA. OSA, characterized by CIH, was shown to cause hypertension (25, 26) and is associated with an increased risk of cardiovascular disease (27, 28). The mechanisms underlying the development of cardiovascular disease in patients with OSA syndromes are poorly understood. The most likely hypothesis is that of a multifactorial process including sympathetic overactivity, selective activation of inflammatory pathways, endothelial dysfunction, and metabolic dysregulation (28). In addition to OSA, ROS-dependent hypoxic response is generated after ischemia-reperfusion that occurs in the treatment of myocardial infarction and stroke. It is accepted that HIF activation confers protection against ischemia-reperfusion injury (29, 30). Although ROS is also generated in various pathological conditions, including hyperglycemia caused by type I and II diabetes (31), it is undefined whether HIF-α up-regulation is associated with increased ROS levels.

Magnesium deficiency is not a rare occurrence and is seen in ~2% of the general population. It is common in patients with diabetes mellitus and alcoholism. It is also common in critically ill patients in intensive care unit settings with a reported prevalence ranging from ~20 to 65% (16). In patients with ischemic heart disease, magnesium deficiency is also frequently found, and this has been reported to be directly related to the disease (13, 15). The present study strongly suggests that magnesium deficiency, which attenuates ROS-dependent hypoxic response, may be a risk factor for the patients suffering from ROS-related diseases such as OSA and ischemia-reperfusion injury, and it could promote the development of complications of the diseases. Magnesium deficiency and ROS have been separately considered to have roles in the etiology of ischemic cardiovascular diseases and ischemic stroke. Our results demonstrate that there is a close linkage between these two pathogenic factors. The mechanism that HIF-1 activity is regulated by extracellular His and Thr is unknown and awaited for clarification.

The present study also suggests that expression of T-type calcium channels may, at least in part, define cell type specificity of magnesium-dependent hypoxic responsibility (Fig. 1B). T-type channels are expressed in several types of excitable cells including neurons in the central and peripheral nervous system, cardiac and smooth muscle cells, and chromaffin cells (19, 32). T-type channels in the nervous system are implicated in the generation of absence seizures, sleep modulation, and pain perception (33, 34), and in cardiac cells they are suggested to be important for cardiac conduction and pacemaking (32). Although T-type channels are also expressed in nonexcitable cells such as vascular endothelial cells, fibroblasts, and cancer cells (32), functions in those cells are largely unknown. T-type channels can be activated by a weak depolarization near the resting membrane potential. There are three genes for the pore-forming α1 subunit of T-type channels, *CACNA1G* for α_{1G}, *CACNA1H* for α_{1H}, and *CACNA1I* for α_{1I}. These three α_1 subunits are expressed differently or concomitantly in various cells (19, 32). It remains to be seen which subunit(s) is responsible for the magnesium-dependent calcium influx. It is interesting to note that the α_{1H} subunit is induced by hypoxia (35).

The present study demonstrates that suppression of ROS-induced hypoxic response may occur in the cells expressing T-type calcium channels such as paraganglion cells in the AM (36) and CB (37). Loss of hypoxic response at the gene level and possible inappropriate activation of the NF-κB target genes in the cells may cause an unwanted and unexpected response, leading to their deteriorate functions. NF-κB activates a variety of genes for immune response, cell adhesion, stress response, cell survival, and oncogenesis (38). In PC12 cells, cooperation of two different signals, one from calcium entry and the other from PI3K, was necessary for NF-κB activation. Activation of IPAS gene expression by the treatment of PMA suggests that PKC is involved in the activation process. An analogous mechanism for NF-κB activation has been known in antigen-stimulated T and B cells (39). In T cells activated by antigen-presenting cells, NF-κB is fully stimulated by two different signals, one from activated T cell receptors binding to antigen and major histocompatibility complex (signal 1) and the other from costimulatory molecules such as CD28 (signal 2). CD28 costimulation mediates up-regulation of PI3K and successively PDK1, which modulates signals through T cell receptors and leads to different cell fates (40, 41). These two signals fully activate PKCθ, which in turn activates CARMA1 to form the CARMA complex (CARMA1, Bcl10, and MALT1), allowing activation of IKK (21, 40, 42). In B cell activation, PKCβ is involved instead of PKCθ. Because of extreme sensitivity of PC12 cells to pharmacological inhibitors of PKC, we are presently unable to identify PKC isotypes that are involved in the up-regulation of NF-κB, although an inhibitor of PKCθ, rottlerin, suppressed the IPAS mRNA induction (supplemental Fig. S5). It is important to know the detailed molecular mechanism by which IKK is activated in PC12 cells and paraganglion cells. Constitutive expression of IPAS was reported in the Purkinje cells of the cerebellum and corneal epithelial

FIGURE 7. **Calcium-dependent molecular mechanism leading to IPAS gene activation.** *A*, the intracellular calcium concentration increased 5 min after CoCl$_2$ treatment in PRMI-cultured PC12 cells. Calcium signaling was monitored using the cells loaded with Fluo-8 AM. The data shown are representative of three experiments. The cells with A23187 treatment for 25 min were used as positive controls. Some cells with A23187 treatment underwent apoptotic DNA fragmentation. *B*, mibefradil (10 μM) inhibited the CoCl$_2$-induced expression of IPAS mRNA (*left* and *middle panels*) and activated HRE-dependent luciferase activity (*right panel*) in RPMI-cultured PC12 cells. *C*, the treatment of 300 μM NiCl$_2$ did not induce IPAS mRNA (*left* and *middle panels*) and partially enhanced HRE-dependent luciferase activity in RPMI (*right panel*). *D*, MK-801 weakly activated the reporter activity in dose dependent manner. *E*, A23187 induced the expression of IPAS mRNA in response to CoCl$_2$ treatment (*left* and *middle panels*) and inhibited HRE-driven reporter activity (*right panels*) in DMEM. *, $p < 0.05$ for indicated comparison. **, $p < 0.01$ for indicated comparison. The data shown in the bar graphs are the averages $\pm$ S.D. of three independent experiments.
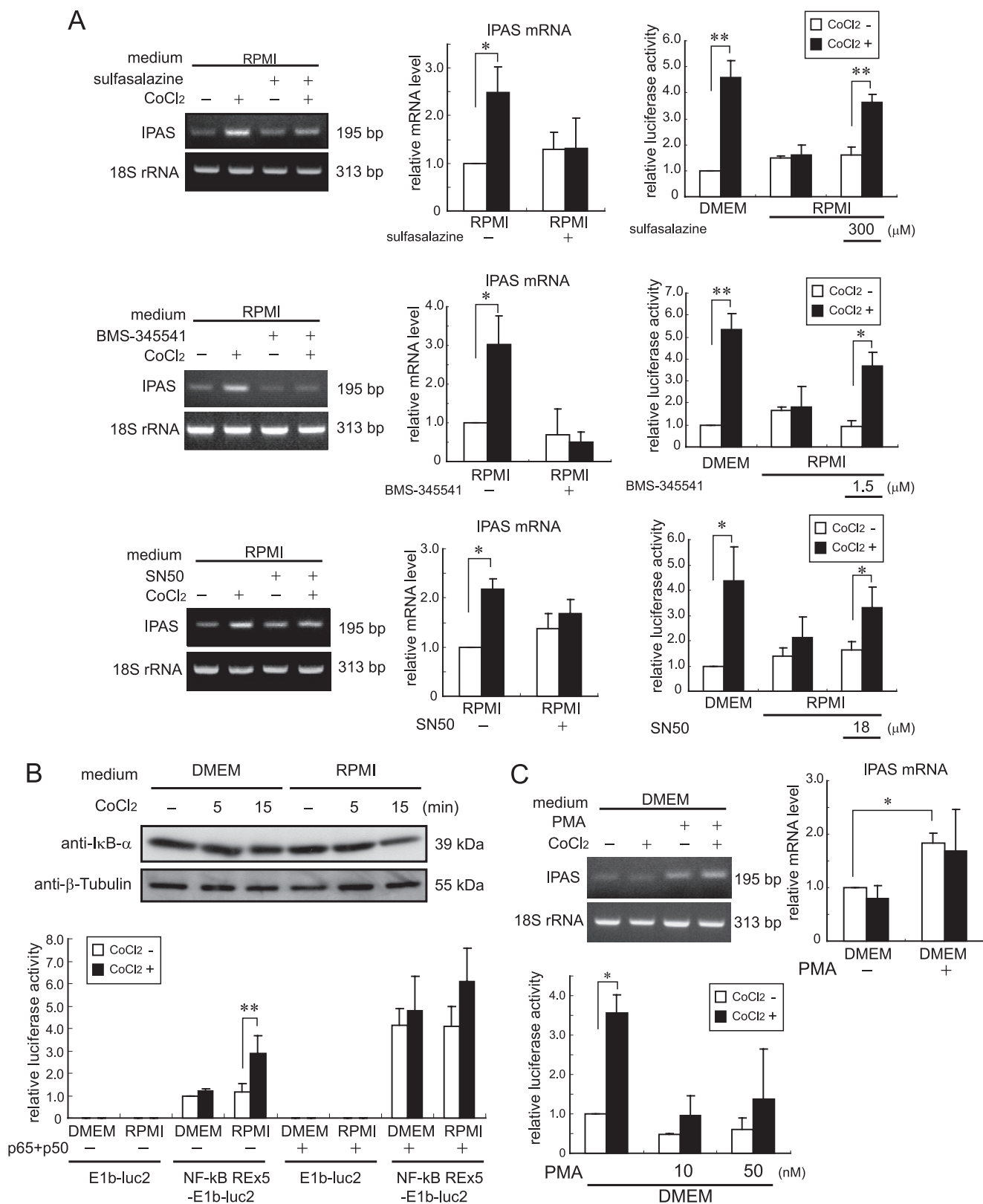
FIGURE 8. **NF-κB signaling-dependent molecular mechanism leading to IPAS gene activation.** *A,* inhibitors of IKK-NF-κB signaling, sulfasalazine (*top panel*), BMS-345541 (*middle panel*), and SN50 (*bottom panel*) blocked IPAS expression and activated the reporter activity. *B,* IκB-α protein declined weakly at 15 min after CoCl₂ treatment in RPMI-cultured PC12 cells. The data shown are representative of three experiments (*top panel*). NF-κB response element-dependent reporter activity was measured by dual luciferase assay system. The luciferase activity was enhanced by CoCl₂ treatment in RPMI-cultured PC12 cells (*bottom panel*). NF-κB complex (p65 and p50) expression enhanced NF-κB response element-dependent reporter activity in both media. *C,* PMA (50 nM) induced the expression of IPAS mRNA regardless of CoCl₂ treatment (*left panel*). PMA inactivated HRE-dependent reporter activity in DMEM (*right panel*). PC12 cells were treated with each drug 30 min before 100 μM CoCl₂ treatment. *, $p < 0.05$ for indicated comparison. **, $p < 0.01$ for indicated comparison. The data shown in the bar graphs are the averages ± S.D. of three independent experiments.

cells (11), and reports demonstrated its inducible expression by hypoxia, creating a negative feedback loop(12). Present study demonstrates that its expression is up-regulated by NF-κB, leading to suppression of HIF-1 activity in at least paraganglion cells under low magnesium environment.

REFERENCES

1. Hirota, K., and Semenza, G. L. (2005) *Biochem. Biophys. Res. Commun.* **338,** 610–616
2. Schofield, C. J., and Ratcliffe, P. J. (2005) *Biochem. Biophys. Res. Commun.* **338,** 617–626
3. Kaelin, W. G., Jr. (2005) *Biochem. Biophys. Res. Commun.* **338,** 627–638
4. Paulding, W. R., Schnell, P. O., Bauer, A. L., Striet, J. B., Nash, J. A., Kuznetsova, A. V., and Czyzyk-Krzeska, M. F. (2002) *Microsc. Res. Tech.* **59,** 178–187
5. Peers, C., and Buckler, K. J. (1995) *J. Membr. Biol.* **144,** 1–9
6. Pardal, R., Ortega-Sáenz, P., Durán, R., and López-Barneo, J. (2007) *Cell* **131,** 364–377
7. Xu, W., Chi, L., Row, B. W., Xu, R., Ke, Y., Xu, B., Luo, C., Kheirandish, L., Gozal, D., and Liu, R. (2004) *Neuroscience* **126,** 313–323
8. Chen, L., Einbinder, E., Zhang, Q., Hasday, J., Balke, C. W., and Scharf, S. M. (2005) *Am. J. Respir. Crit. Care Med.* **172,** 915–920
9. Peng, Y. J., Yuan, G., Ramakrishnan, D., Sharma, S. D., Bosch-Marce, M., Kumar, G. K., Semenza, G. L., and Prabhakar, N. R. (2006) *J. Physiol.* **577,** 705–716
10. Hui, A. S., Striet, J. B., Gudelsky, G., Soukhova, G. K., Gozal, E., Beitner-Johnson, D., Guo, S. Z., Sachleben, L. R., Jr., Haycock, J. W., Gozal, D., and Czyzyk-Krzeska, M. F. (2003) *Hypertension* **42,** 1130–1136
11. Makino, Y., Cao, R., Svensson, K., Bertilsson, G., Asman, M., Tanaka, H., Cao, Y., Berkenstam, A., and Poellinger, L. (2001) *Nature* **414,** 550–554
12. Makino, Y., Uenishi, R., Okamoto, K., Isoe, T., Hosono, O., Tanaka, H., Kanopka, A., Poellinger, L., Haneda, M., and Morimoto, C. (2007) *J. Biol. Chem.* **282,** 14073–14082
13. Turlapaty, P. D., and Altura, B. M. (1980) *Science* **208,** 198–200
14. Altura, B. M., Altura, B. T., Gebrewold, A., Ising, H., and Günther, T. (1984) *Science* **223,** 1315–1317
15. Rude, R. K. (1998) *J. Bone Miner Res.* **13,** 749–758
16. Tong, G. M., and Rude, R. K. (2005) *J. Intensive Care Med.* **20,** 3–17
17. Sogawa, K., Numayama-Tsuruta, K., Ema, M., Abe, M., Abe, H., and Fujii-Kuriyama, Y. (1998) *Proc. Natl. Acad. Sci. U.S.A.* **95,** 7368–7373
18. Delpiano, M. A., and Altura, B. M. (1996) *FEBS Lett.* **394,** 335–339
19. Perez-Reyes, E. (2003) *Physiol. Rev.* **83,** 117–161
20. Lee, J. H., Gomora, J. C., Cribbs, L. L., and Perez-Reyes, E. (1999) *Biophys. J.* **77,** 3034–3042
21. Spitaler, M., and Cantrell, D. A. (2004) *Nat. Immunol.* **5,** 785–790
22. Ke, Q., and Costa, M. (2006) *Mol. Pharmacol.* **70,** 1469–1480
23. Chachami, G., Simos, G., Hatziefthimiou, A., Bonanou, S., Molyvdas, P. A., and Paraskeva, E. (2004) *Am. J. Respir. Cell Mol. Biol.* **31,** 544–551
24. Griguer, C. E., Oliva, C. R., Kelley, E. E., Giles, G. I., Lancaster, J. R., Jr., and Gillespie, G. Y. (2006) *Cancer Res.* **66,** 2257–2263
25. Nieto, F. J., Young, T. B., Lind, B. K., Shahar, E., Samet, J. M., Redline, S., D'Agostino, R. B., Newman, A. B., Lebowitz, M. D., and Pickering, T. G. (2000) *Jama* **283,** 1829–1836
26. Peppard, P. E., Young, T., Palta, M., and Skatrud, J. (2000) *N. Engl. J. Med.* **342,** 1378–1384
27. Shamsuzzaman, A. S., Gersh, B. J., and Somers, V. K. (2003) *Jama* **290,** 1906–1914
28. Parati, G., Lombardi, C., and Narkiewicz, K. (2007) *Am. J. Physiol. Regul. Integr. Comp. Physiol.* **293,** R1671–1683
29. Natarajan, R., Salloum, F. N., Fisher, B. J., Kukreja, R. C., and Fowler, A. A., 3rd (2006) *Circ. Res.* **98,** 133–140
30. Loor, G., and Schumacker, P. T. (2008) *Cell Death Differ.* **15,** 686–690
31. Ha, H., Hwang, I. A., Park, J. H., and Lee, H. B. (2008) *Diabetes Res. Clin. Pract.* **82,** S42–S45
32. Yunker, A. M., and McEnery, M. W. (2003) *J. Bioenerg. Biomembr.* **35,** 533–575
33. Bourinet, E., Alloui, A., Monteil, A., Barrère, C., Couette, B., Poirot, O., Pages, A., McRory, J., Snutch, T. P., Eschalier, A., and Nargeot, J. (2005) *EMBO J.* **24,** 315–324
34. Shin, H. S., Cheong, E. J., Choi, S., Lee, J., and Na, H. S. (2008) *Curr. Opin. Pharmacol.* **8,** 33–41
35. Del Toro, R., Levitsky, K. L., López-Barneo, J., and Chiara, M. D. (2003) *J. Biol. Chem.* **278,** 22316–22324
36. Vinet, R., and Vargas, F. F. (1999) *Am. J. Physiol.* **276,** H1313–H1322
37. Caceres, A. I., Gonzalez-Obeso, E., Obeso, A., Gonzalez, C., and Rocher, A. (2007) *Acta Physiol.* **190,** (suppl.) 655
38. Pahl, H. L. (1999) *Oncogene* **18,** 6853–6866
39. Schmitz, M. L., Bacher, S., and Dienz, O. (2003) *FASEB J.* **17,** 2187–2193
40. Lee, K. Y., D'Acquisto, F., Hayden, M. S., Shim, J. H., and Ghosh, S. (2005) *Science* **308,** 114–118
41. Parry, R. V., Riley, J. L., and Ward, S. G. (2007) *Trends Immunol.* **28,** 161–168
42. Springael, C., Thomas, S., Rahmouni, S., Vandamme, A., Goldman, M., Willems, F., and Vosters, O. (2007) *Biochem. Pharmacol.* **73,** 515–525